Numerical Study on Parameters Affecting the Structure of Scaffolds Prepared by Freeze-Drying Method

Madelatparvar, Mahdi; Salami Hosseini, Mahdi*[+•]; Abbasi, Farhang[•]

Faculty of Polymer Engineering, Sahand University of Technology, Sahand New Town, Tabriz, I.R. IRAN

ABSTRACT: *Freeze-drying is one of the most used methods for preparing scaffolds and is very sensitive to the material and operational parameters such as nucleation temperature, thermal properties of the mold, cooling rate, set freezing point, and slurry height. In the present study, a Finite Element Method (FEM) based code was developed to investigate the effects of such parameters and to eventually predict the microstructure of the scaffold. Similar molds and cooling conditions used in various experimental studies were simulated and compared. The achieved pattern demonstrated how different thermal condition tailored scaffold microstructure. It was shown that nucleation temperature (T_n) was an effective parameter controlling the final structure of the scaffold and influenced pore sizes with different mold materials. Simulation results also showed that by decreasing the rate of cooling, the average pore sizes increased, and a quenching solution led to a randomly distributed pattern of pore sizes. It is also achieved that by increasing the set freezing temperature as well as the height of the solution the pore sizes increased more at the top of the mold. The thermal gradient also illustrated the orientation of the pore in a mold with the thick isolated wall was considerably uniform. This framework can be used to optimize the scaffold structure or any ice templating method.*

KEYWORDS: *Finite element methods; Scaffold; Freeze-drying; Ice; Crystal size.*

INTRODUCTION

The development of tissue engineering has increased the need for biocompatible scaffolds since they are used widely in healing patients suffering from tissue loss. Scaffolds are sponge-like materials with a high and interconnected porosity which can act as external cellular matrices [1]. Among all the factors influencing cells attachment, growth and differentiation in a scaffold, pore size, shape and orientation have the greatest impact on the scaffold performance and are thus principal challenges for researchers. Therefore, tailoring scaffold to achieve appropriate architecture is considered a substantial task in tissue engineering [2].

In spite of the advent of various scaffold fabrication methods, there is an increasing tendency to fabricate scaffolds through freeze-drying. As a simple method that uses no chemicals, freeze-drying has become one of the most conventional and wildly accepted methods of scaffold fabrication, and studying the morphology of obtained scaffolds has grown in recent years [3-8]. In this method, a dilute water/polymer solution is frozen

** To whom correspondence should be addressed.*

+ E-mail: salami@sut.ac.ir

• Other Address: Institute of Polymeric Materials, Sahand University of Technology, Sahand New Town, Tabriz, I.R. IRAN

1021-9986/2020/2/273-288 16/$/6.06

under a specific condition, and the frozen cake is lyophilized under the vacuum and below the melting point of water. In freezing step, the ice crystals begin to grow dendritically from nuclei inside the solution. As the water crystal size increases, polymer phases are pushed away and concentrate. This causes water crystals to form an interpenetrating network between the very fine layers of polymer. When the crystallization is finished, two separate phases (consisting of ice and polymer) are formed from the primary solution. Ice sublimation in drying step fixes the layer structure. On its own, this is a notable technique known as ice-casting or ice templating [9]. The freezing step plays the main role in tailoring the scaffold, because in this step, crystals are formed and the structure is solidified. Therefore, to reach the desirable structure, especially in terms of pore pattern and size, such parameters as cooling rate, set freezing point, and slurry height should be adjusted during the freezing stage.

The general pattern achieved by freeze-drying varies, from the axially oriented anisotropic morphology to the spherical shape with interconnected pores, where the former has the potential to be applied in the treatment of peripheral nerves and spinal cord [10], and the latter can be used frequently in derma applications as well as conjunctiva treatment [11-12].

The mean scaffold pore size is a further subject of interest, because of its effects on cells. As such, decreasing the pore size can maximize specific surface of the scaffold allowing it to contain more cells, while pore size is kept large enough to let the cells migrate into the scaffold [13]. Moreover, cell attachment and migration depend on the size and curvature of the pores [14]. As a result, the scaffold pores should be tailored to cell culture, which is only possible while the ice crystal growth is controlled locally within the slurry through the aforementioned freezing parameters.

The growth of the crystals in each direction is heavily dependent on the temperature differences between the tip of the crystal and its adjacent surrounded area [15]. Therefore, there is a high demand to get detailed information on the heat transfer and temperature profile in the mold, which could allow for prediction the pore structure of the scaffold. Many experimental researches have been carried out to obtain the temperature profile and find its relationship with the scaffold pore size and orientation [6, 16-17]. O'Brien et al. studied the effect of freezing rate on the size of the pores [3], and Madaghiele et al. followed by producing an axially oriented scaffold [4]. Haugh et al. suggested a new method to gain different pore sizes [7] by altering the final freezing temperature and annealing. Davidenkov et al. employed different molds for making scaffold [6] and Pawelec et al. studied the effect of increasing the slurry height in the mold and set freezing temperature on the pore size of the scaffold at the top and base [17]. The recent authors used recorded thermal profile by thermocouple to study and control resulting scaffold architecture. However, the simulation of freeze-drying and predicting the final scaffold structure has received less attention. As the experimental investigation of the nucleation temperature and molding conditions are highly complex and the results are not reproducible, simulating of the effects of such parameters seems necessary.

The inherent intricacies of such a study are rooted in the complexity of water crystallization [18-20] and the stochastic nature of nucleation phenomena [17, 21]. Simulation allows all parameters to be analyzed precisely and independently. Nevertheless, a small number of studies have been devoted to find a suitable model to predict the crystals structure in the freeze-drying process [22]. *Nakagawa et al.* proposed a method to determine the ice crystal mean size during freezing pharmaceutical formulation in vials using the simulation of temperature profile [21]. Muzzio et al. obtained ice crystal size distribution in a freeze-dried drug by simulating the freeze-drying process through the Finite Element Method (FEM) [23]. *Nakagawa et al.* obtained an empirical relationship between freezing front velocity and the temperature gradient in the frozen zone with the ice crystal morphology [24]. *Ortega et al.* modeled crystallization with Eulerian model for the temperature profile and predicted the crystal size through the population balance model [25].

Furthermore, simulation has been used to estimate the mechanical properties of scaffold [26-27]; to study the angiogenesis and vascularization in terms of the various scaffold architecture [28] and to investigate the flow dynamic throughout different porous scaffolds [29-32]. Such studies mainly use uniform porous structures or random placement of pores which are not the results of freeze-drying method. However, a structural scaffold model simulated through mechanistic approach based on crystallization capable of utilization in such studies is absent from the literature. Aside from this, a simulation of scaffold fabrication in order to find relationships between morphological structure and freezing conditions such as

employing different molds, could assist the optimization of scaffold architecture and fabricating any desirable structure. This could be usefulconsidering recent attention to structure of the freeze-dried scaffolds.

The objective of the present study is to investigate the effect of operational and material parameters on the scaffold structure and predict the pore size and its distribution pattern in a freeze-dried scaffold formed *via* ice templating. For this purpose, a finite element code was developed to capture the temperature distribution and simulate the freezing process of the slurry, which was then used to estimate the scaffold structure using an empirical model. Experiments were also performed to estimate ice crystal size and eventually the scaffold pore size.

EXPERIMENTAL SECTION

Scaffold preparation

Gelatin scaffolds were fabricated through the freeze-drying method instructed by the procedure described in *Abbasi et al.* [33]. An aqueous solution of 3% gelatin was prepared by solving gelatin powder (Merck, Schuchardt, Germany, used as received) in distilled water. The solution was stirred using a magnetic stirrer for 30 min at 55 °C, mixed, and centrifuged in a bench-top centrifuge at 5000 rpm for 15 min to remove air bubbles. The prepared slurry was poured into the mold and placed in a freezer chamber at room temperature. The temperatures of the freezer chamber were decreased by a constant rate of 0.9 °C/min until it reached –40°C and held at this temperature. Two frozen samples were then lyophilized using a freeze-dryer equipment (Operon model FDU8606, South Korea) for 24 h at 0 °C, in vacuum condition (<100 mTorr).

Pore size determination

Samples were cut by a very sharp blade to obtain a clean cross-section to study the pattern of pore size from a vertical cross-section area of the scaffold. An optical microscope (Olympus IX71, Japan) was employed to capture the micrograph from the cross-section. The images were analyzed using the image analysis software, ImageJ, to determine the pore size, and pore size distribution pattern was compared to simulated results.

THEORETICAL SECTION

Numerical procedure

A two-dimensional axisymmetric finite element model was employed to simulate the heat transfer process in the mold and a proper code in MATLAB was developed. Due to the symmetry of the geometry, a 2D geometry of the cross-section of the mold, as shown in Fig. 1(a), was discretized using 4-node quadrilateral linear elements and an implicit scheme was employed to discretize the time space. A various number of elements were used to discretize the computational domain and finally, 1000 elements was chosen based on the mesh independence study and optimization of the calculation cost. The employed geometry and mesh is presented in detail in Fig. 1(b). Since the concentration of gelatin in water was very low (less than 3%), the slurry material was considered as pure water and ice, as well as a mixture of them during the phase change and its properties were applied accordingly. The governing equation of the heat transfer is presented in Equation (1):

$$\rho C_p \frac{\partial T}{\partial t} = \lambda \nabla^2 T + \dot{q}_{cr} \quad (1)$$

where ρ,C_p, t, T, $\dot{q}_{cr}$ and λ respectively represent density, heat capacity, time, temperature, volumetric heat generation per time (specific latent heat) and heat conductivity. and was considered to be subjected to the following boundary condition, on exposed boundary to the freezer atmosphere:

$$-\lambda \nabla T.\, n = h\,(T - T_\infty) \quad (2)$$

In which n, h and T_∞ respectively represent normal vector of the boundary, convection heat transfer coefficient and ambient temperature. The values of the heat transfer coefficient, *h*, were calculated through the model proposed for the free convection by *William et al.* [34] for different mold surfaces, and are presented in Table 1 for different molds

The approach proposed by *Muzzio et al.* [23] was employed to take into account the effect of latent hea.. In this approach, each element was considered to take one of the following three states: liquid Water State (WS), Ice State (IS) or ice and water Mixture State (MS). Each element was first considered to be WS until it reaches nucleation temperature or at least one of its neighbors are in IS. In any such situation, the element is turned into MS with the properties of the mean of IS and WS. The element remains in MS as long as the integrated transmitted heat through the elements reaches the fixed thermodynamic quantity, *Q*, which can be defined as follows:

$$Q = \Delta H_f . V_{elem} \quad (3)$$

Table 1. Material properties

Material property	Value	Unit
λ (aluminum)	237	W/m°K
λ (polystyrene)	0.3	W/m°K
λ (water)	0.60	W/m°K
λ (ice)	2.10	W/m°K
λ (air)	0.02	W/m°K
C_p (aluminum)	452,000	J/m^{3o}K
C_p (polystyrene)	2,300,000	J/m^{3o}K
C_p(water)	4,220,000	J/m^{3o}K
C_p (ice)	2,000,000	J/m^{3o}K
C_p (air)	1206	J/m^{3o}K
α (aluminum)	8.418 × 10e-5	m^2/s
α (polystyrene)	0.107 ×10e-6	m^2/s
ΔH_f	333,500	J/kg
h aluminum to air	15	W/m^{2}k
h polystyrene to air	12	W/m^{2}k
h water to air	6	W/m^{2}k
k (pore size estimation)	5.432 10e-5	-

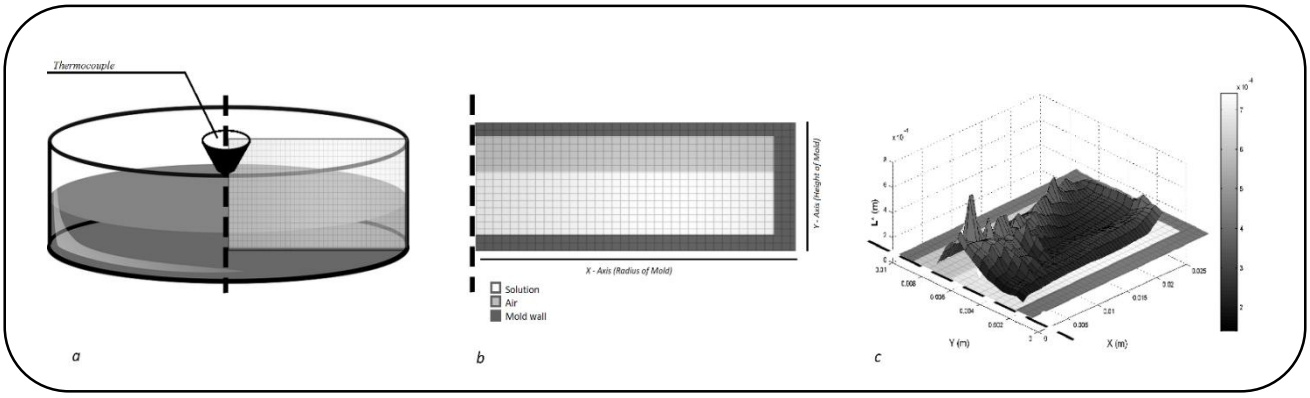

Fig. 1: (a) Schematic design of the mold, (b) Discretized 2D domain, (c) typical predicted distribution of the pore size (x-axis: central mold line, y-axis: bottom of the mold, z-axis: average pore sizes).

Where ΔH_f is the heat of fusion of water and V_{elem} is the element volume. The period of time each element needs to reach Q is considered as its solidification time, t_s, and is stored to calculate the crystal size later.

Determining crystal size

In order to determine the expected crystal size in the mold, the model proposed by *Nakagawa et al.* [24] was employed in the present work. In the model, the correlation between freezing parameters and crystal size was proposed as:

$$L^* = k\, G^{-0.2} R^{-0.2} \quad (4)$$

where, L^*, k, G and R represent the crystal mean size, correlation constant, magnitude of temperature gradient and freezing front velocity, respectively. The mean ice

crystal is represented topologically on the 2D cross section of the scaffold (Fig. 1(c)). *k* is an empirical constant which was obtained through experiment. Velocity of freezing front in x- and y-direction (R_x and R_y), for each element could be calculated as:

$$R_x = \frac{H_{elem}}{t_s} \quad (5a)$$

$$R_y = \frac{L_{elem}}{t_s} \quad (5b)$$

$$R = \sqrt{R_x^2 + R_y^2} \quad (5c)$$

Where t_s, L_{elem} and H_{elem} are the freezing time, length and height of the element, respectively. Since the temperature of the element is constant during freezing process, using the standard finite element procedure to calculate the temperature gradient in the element will result in inconsistent results. To overcome this issue, the temperature gradient vector was estimated for the i-th element by determining the mean temperature difference of its center and adjacent elements in x- and y-direction. Finally, the norm of the gradient vector was considered as *G* in Equation (3).

RESULTS AND DISCUSSION

Temperature profile

In agreement with reported experimental and simulated results [6, 16, 21, 23], predicted temperature profile went through three different stages; First, before the nucleation commenced, each element inside the slurry cooled according to its location and the mold condition in freezer. As the element temperature reached nucleation temperature, T_n, generation of latent heat in the element occurred, fixing the temperature of the element at melting temperature, T_m, while other parts of the slurry volume were in liquid state at various temperatures. Finally, all parts crystallized and the temperature of the slurry decreased to reach the temperature imposed by the ambient air inside the freezer (Fig. 2).

It should be noted that the temperature plateau duration, i.e. solidification time (t_s), for each element is necessary for calculating the crystal size in the element which can be used to estimate the pore size of the final scaffold. Depending on the state of the neighbors and condition of elements, each element showed different thermal plateau (i.e. solidification time) which was depended directly to the temperature and the state of the adjacent elements. The more the temperature differences among adjacent elements, the shorter the freezing plateau. In contrast, the freezing process with small temperature differences between adjacent elements occurred slowly leading to the generation of bigger pores.

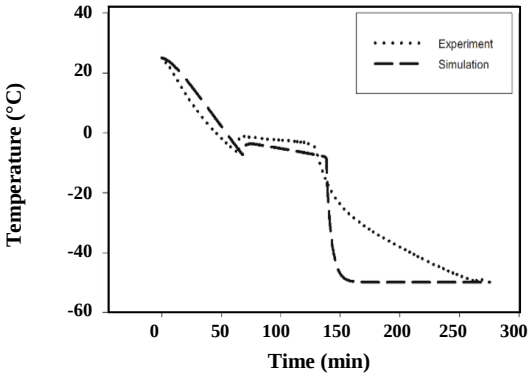

Fig. 2: Comparison of the simulated and experimental result of the slurry temperature. ($T_n = -7$ °C, height of slurry = 6 mm).

Comparing the experimental and simulated results depicted that there was difference especially in the final stage of freezing where simulated results showed a sudden decrease after freezing. One reason for such an observation could lie on the temperature recorded by thermocouple where it measured the temperature of a limited region instead of the exact temperature of a certain point. As the size of the sensor used to record the temperature variation was comparable to mesh size, only the average temperature of the region around the sensor, instead of a certain point, was recorded which can be interpreted as the average temperature of that region. Nevertheless, simulated results reflected the very temperature of a certain point of the slurry in the mold. Thus, the difference between the experimental and simulated results was expected. Moreover, the heat transfer coefficient was calculated using the model proposed by *Williams et al.* [34] which could be somehow different with the actual one in the freezer used for the experiment. However, it should be noted that the solidification/freezing time, t_s, and overall trend of the temperature variation within the mold were predicted accordingly, which was confirmed by the results of experimental pore size distribution.

The effect of nucleation temperature (T_n)

It has been always tried to control the formation of the ice crystal structure in freeze-drying process to get

a porous material having a desired structure. One of the problems in controlling the ice templating technique is the stochastic nature of ice nucleation during the supercooling of water. Due to the fact that the nucleation of ice occurs in different time and temperature, the formation of ice crystals structures varies, which means that different structures are made by the same cooling condition and operational parameters. Hence, the effect of nucleation temperature, T_n, could not be investigated experimentally. Nevertheless, simulation techniques provide a tool to study the effect of parameters which are not experimentally controllable. In order to study the effect of T_n on the pore size of the scaffold prepared by freeze-drying process, T_n was considered as a fixed value between −1.5 °C, i.e. near the freezing temperature, and −10 °C, based on our experimental conditions for two different molds and its effect on the final pore size were investigated.

The effect of T_n in the polystyrene mold

In order to study how different T_n alter the scaffold structure and average pore size, different T_n, -2.5 and -7 °C, were taken into account and the resulting crystal structures were predicted in the same cooling condition which are illustrated in Fig. 3 (a) and (b). It can be seen that scaffold structures consisted of small pore size in the center and slightly bigger pore size near the mold side wall. It could be seen that pore size in the center of the scaffold increased as T_n increased. More precisely, statistic measurement showed the average pore size decreased steadily from 160 to 149 μm as T_n decreased from −2.5 to −7 °C (Fig. 4(e)).

According to the results presented in Fig. 3 (a), lower T_n accelerated the freezing process and led to the reduction of the average pore size since the crystals had shorter time to grow. As polystyrene had very low thermal conductivity, the released latent heat of water accumulated inside the mold so the condition of heat transfer process remained almost alike for different T_n resulting in a similar crystal size distribution.

The effect of T_n in the aluminum mold

For aluminum mold, altering T_n had a different effect on the pattern of the crystal (i.e., pore) size distribution. As shown in Fig. 4 (a), at T_n = -7 °C, there was a bigger pore size around the slurry mainly at the top of the mold. This pattern was changed when T_n was equal to -5 °C (Fig. 4 (b), where the bigger pore size appeared at the center of the scaffold and scattered at the top. In higher T_n (i.e. T_n = – 2.5°C), as shown in Fig. 4 (d), the scaffold morphology became similar to the polystyrene mold, but with a significant difference in pore size. Comparing the results to ones obtained in PS mold showed that altering T_n had a dramatic effect on the final crystal/pore size distribution in the aluminum mold which was in accordance with our experience. It means that scaffolds fabricated by the PS mold showed more reproducibility than that prepared using the aluminum mold. Moreover, it was seen that the average crystal/pore size in the aluminum mold was much bigger than that was seen for the PS mold and the trend was quite different (Fig. 5). Experiment also performed to investigate the compatibility of the obtained pattern in this case (i.e. aluminum mold). Fig. 6 shows a well compatibility of the pattern in the same condition.

To interpret these results, one should focus on the heat conductivity of Aluminum. Higher heat conductivity of Aluminum assisted the heat to transfer from generating locations to the other areas within the mold, homogenizing the temperature distribution. This, in turn, led to increase the time of solidification, as a result of decreasing temperature differences. Bigger pore/crystal sizes obtained from aluminum mold was the direct result of the crystallization time increment.

It should be mentioned that crystallization procedure was influenced by other factors such as concentration gradient of slurry as well as surface roughness of the mold which were not considered in the current study and may disrupt the actual occurrence of this outcome. However, it can be concluded from Fig. 6 that experimental data supported the simulated pattern.

As mentioned before, the simulation was conducted considering the mold and conditions employed by *Ghale et al.* [33] and the final simulated results were compared to ones reported experimentally by them (Fig. 7). Since different nucleation temperatures led to different pore sizes, the simulated pore size reported in the present study was considered as the average of pore sizes predicted by considering T_n varying from –2 to –8 °C. Fig. 7 compares the simulated results of two set freezing points and different mold material. It can be noticed that the simulation results for aluminum mold at –40 °C showed very good compliance with the experimental results since L* was directly measured from the very same

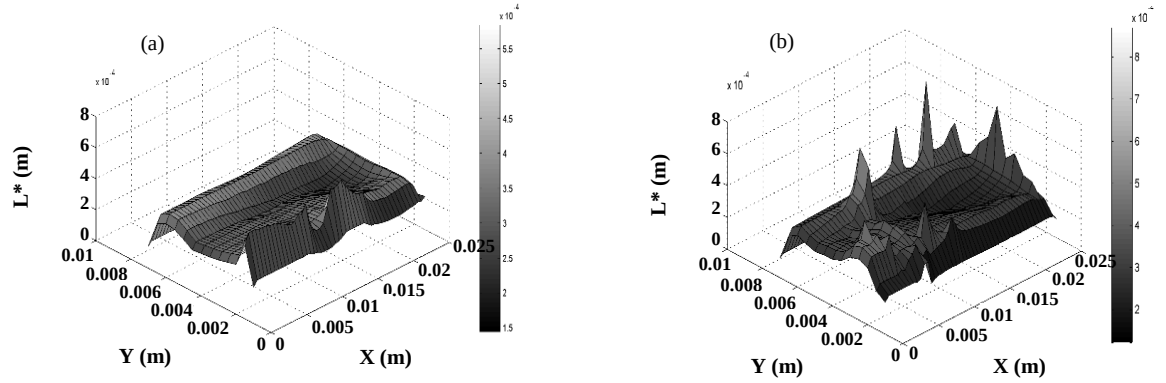

Fig. 3: Pattern of calculated pore size in polystyrene mold with different T_n: (a) T_n = –7 °C (b) T_n = –2.5 °C.

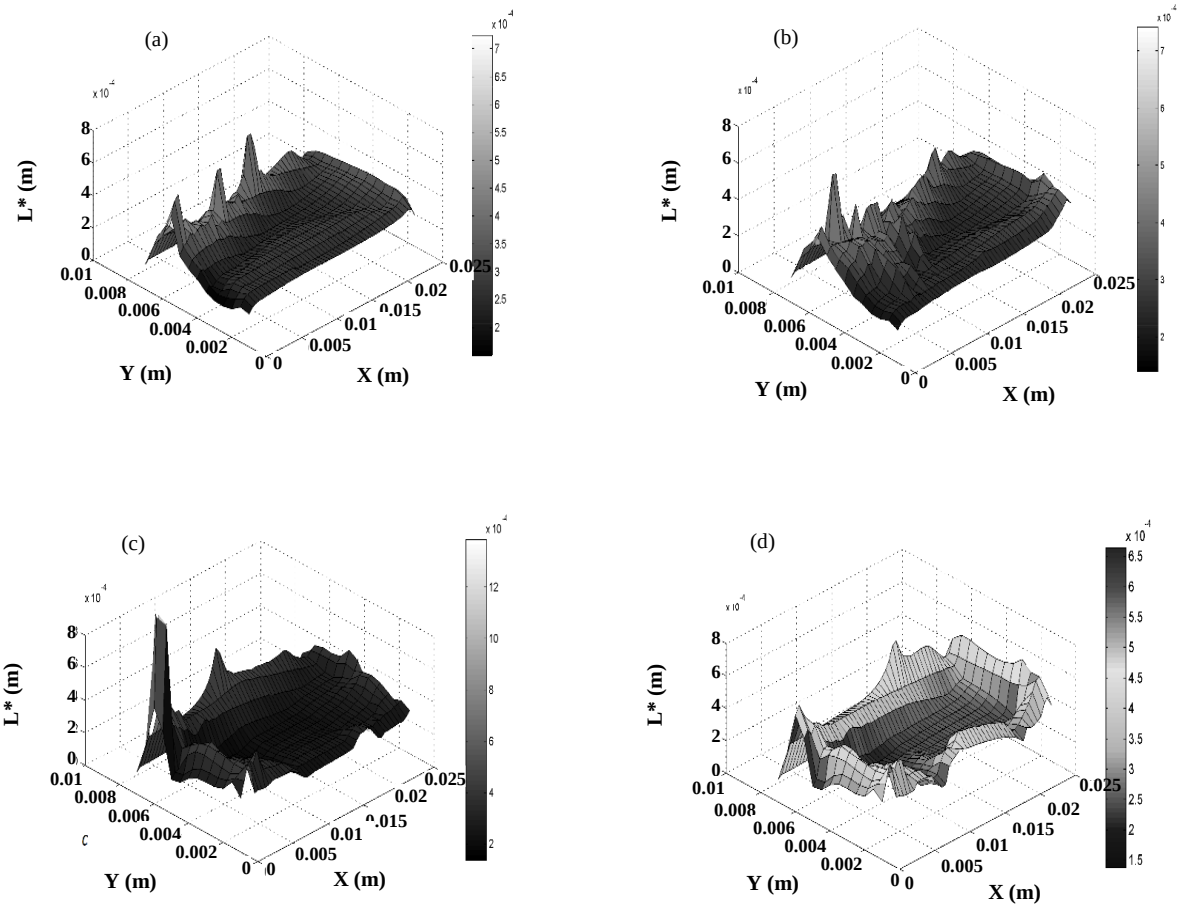

Fig. 4: Pattern of calculated pore size in aluminum mold with different T_n; (a) T_n = –6.5 °C (b) T_n = –5 °C (c) T_n = –3 °C (d) T_n = –2.25 °C.

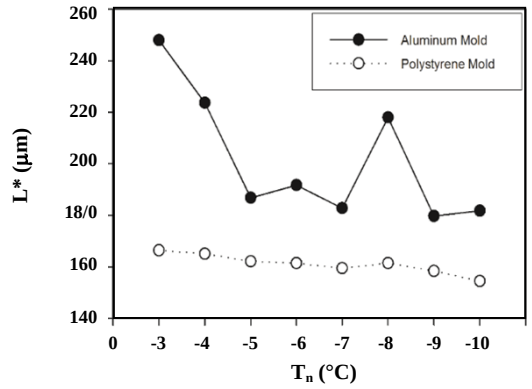

Fig. 5: Comparison of average pore size in Al and PS mold in different set freezing temperature.

experimental condition. Using different molds with different freezing conditions might lead to have different *k* values. However, for the sake of simplicity and comparison, the same value of *k* was used to predict the pore/crystal size for different molds with different freezing conditions. According to Fig. 5, it should be noted that as the freezer temperature decreased, the pore/crystal size decreased, being the direct result of a high heat transfer rate and shortening the solidification time, t_s. It can be seen that the pore/crystal size was smaller in PS mold compared to one obtained in Al mold which was observed experimentally and theoretically. This could be explained in term of difference of the heat conductivity of aluminum and polystyrene which was discussed in previous sections. The non-conformity between simulated and experimental data of the average pore size in Al mold by set freezing point of -80 °C might be due to the effect of the nucleation temperature which was not considered in the experimental result.

The effect of cooling rate

The effect of different cooling conditions were studied by employing four different cooling conditions, 0.9, 0.7, and 0.6 °C/min and quenching at –40°C, and results were compared to the reported ones by *O'Brien et al.* [3] (see Figs. 8 and 9). The simulated results showed the same trend as observed in the experimental data provided by *O'Brien et al.* [3], but with an exception in the absolute pore size. The difference in the pore size could be related to the correlation factor, *k*, used to calculate the crystal size in Equation 4. Since the same mold was not available for further studies, the correlation factor of the used mold in previous sections with the same material was considered which could be the source of this difference. Also, it was believed that quenching would normally decrease the crystal/pore sizes, while *O'Brien et al.* [3] showed that quenched sample 4.1 had bigger pores than 0.9. Although it was not obtained exactly in simulation results, pore sizes were similar in 0.9 and 4.1.

It was revealed that the scaffold prepared by constant cooling rate of 0.9 °C/min had the minimum average pore sizes of 157 µm among those prepared by constant cooling rate. In contrast, the maximum average pore sizes were obtained by cooling rate of 0.6 °C/min, 166 µm which was similar to the achieved trend in experimental results by O'Brien et al. [3]. Because higher cooling rates took out the generated latent heat faster than lower ones, it could lead to shorten the solidification time, t_s, and reduce the crystal/pore size. Holding the same pattern, pore/crystal size decreased, as the cooling rate increased, which indicated the resembling reduction of t_s throughout the slurry.

According to the simulation results, scaffolds fabricated using the constant cooling rate (0.9 and 0.6 °C/min), Fig. 8, showed more uniform structure than those obtained through quenching process. This inconsistency could be seen in the pore size distribution center during the slurry cool-down through the quenching method (Fig. 8(c)). This is mainly due to simultaneous nucleation occurred during constant cooling rate and ice crystals then formed uniformly throughout the slurry [8].

It was also reported [3] that the quenching process led to an average pore size of 110 µm, which placed between the average scaffold pore size values prepared by constant freezing rate of 0.9 and 0.7 °C/min, whereas simulation results of quenching method showed the smallest pore size due to the highest cooling rate of the quenching method (i.e. 4.1 °C/min). It seems that the case simulated corresponds to the limit case when the ice growth in the slurry is slow and freezing front is close to zero [25] (Fig. 9).

The Effect of set freezer temperature

Changing the set freezing temperature led to change in pore size at the top and base of the scaffold. In order to compare the predicted results with experimental ones, the cooling conditions of mold as well as its geometry were considered similar to those [17] employed in experimental study (Table 2). Indeed, in order to compare the average pore size of the top and bottom of the scaffold,

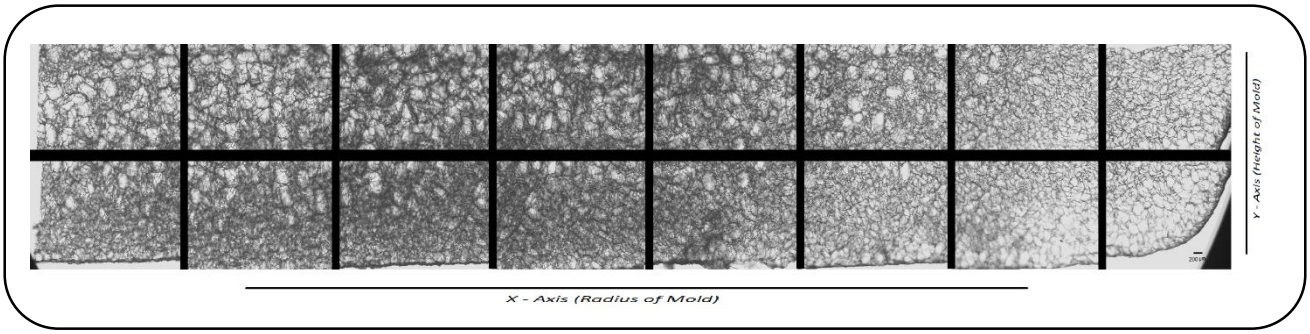

Fig. 6: Experimental results of the distribution of the pore sizes in the aluminum mold (X- axis is the radius of the mold = 25 mm, Y- axis = the height of the mold = 6 mm) k was calculated through comparison of this result and simulated result in Fig 1. (a)

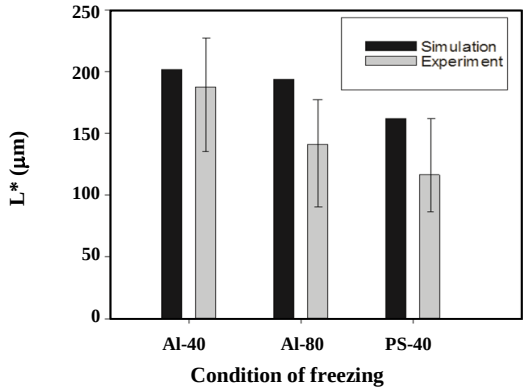

Fig. 7: Comparison of estimated the average pore size and experimental results [33] in aluminum and polystyrene molds in two different set freezing points (height of slurry = 3 mm, average pore size for T_n of –3 to –10 °C).

to separated regions were considered; from the bottom of mold to the half of the scaffold height and from the half height to top of the scaffold. To avoid the influence of higher and lower T_n on the slurry structure in different set freezing point, in this case T_n was set at −7°C which is an average between −3°C and −10°C.

Fig. 10 (a), (b), (c) and (d) show that calculated pore size at the top of the scaffold steadily decreased, as the set freezing temperature decreased while the structure of the bottom did not change. The calculated average pore size for set freezing point of −10 was 220 µm at the top which was near to those reported by Pawelec et al. [17], 197 µm. Other calculated pore size at set freezing points of −20, −30, and −40 at the top had the same compliance with experimental ones. At the bottom of the mold, however, calculated pore size was as doubled as experimental, 200 µm and 100 µm respectively, and decreased as set freezing point decreased.

The differences between experimental and simulation results can be explained by two reasons. Firstly, thermal hold condition could not be simulated completely in the freezing condition, and therefore the set freezing point was set to -10 °C in the simulation which was different from thermal hold condition in experiment. Secondly. It should be noted that in this test, T_n was set to −7 °C which was different from ones observed in experiment, −3 and −10 °C at the top and base respectively. As a result, the calculated pore size at the scaffold base did not match with experimental ones. *Pawelec et al.* [17] showed that the nucleation temperature was affected in different set freezing points and especially in thermal hold condition.

In all different set freezing temperatures, bigger pores were observed mainly at the top which was due to the mold geometry. The insulating properties of polystyrene prohibited the cooling from side wall and instead the bottom and top of the slurry would be cooler and thus, nuclei first, formed in those two cooler areas. After nucleation began, the top and bottom of the slurry became warmer. The latent heat was then transferred through the convection of the ambient air at the top and the steel bottom whose convection heat transfer coefficient was as doubled as the top air (see Table 1). It caused the freezing time at the top increased. Moreover, as there was the smaller temperature gradient between mold and shelf in higher set freezing point, nuclei had more time to grow and consequently pore size became bigger specifically in the top and bottom of slurry.

The effect of the slurry filling height

Increasing the slurry filling height in the mold had a notable effect on the pore size distribution. It was believed that the variation of pore/crystal size in the mold with different slurry filling heights depended

Table 2: Cooling conditions and mold geometry in tests.

Section	Mold geometry	Cooling condition
3.3	original steel pan (12 cm × 12 cm)	ramped cooling by a rate of 0.9, 0.7, and 0.6 °C/min and holding at –40 °C and the quenching technique, i.e. putting mold in precooled freezer at the set freezing point of –40 °C (4.1 °C/min)
3.4	Steel cylindrical mold with a thick Perspex wall (inner radius = 11 mm, height = 30 mm, side wall thickness = 9 mm	cooling rate = 0.9 °C/min and final set freezing temperature = –10, –20, –30 and –40 °C
3.5	as same as 3.4	cooling rate = 0.9 °C/min and final set freezing temperature = –30 °C)

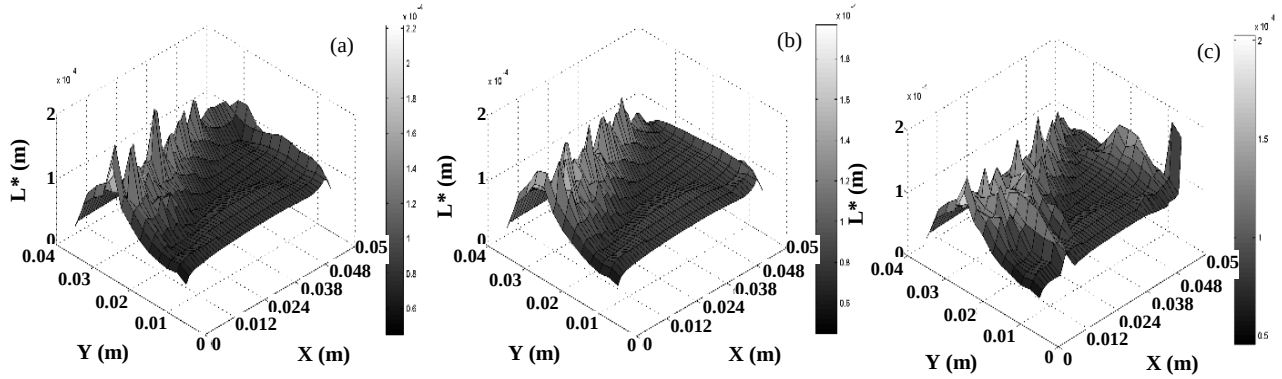

Fig. 8: The pore size distribution at different cooling rate of (a) 0.9 °C/min and (b) 0.6 °C/min, (c) quenching method executed at set freezing point of –40 °C

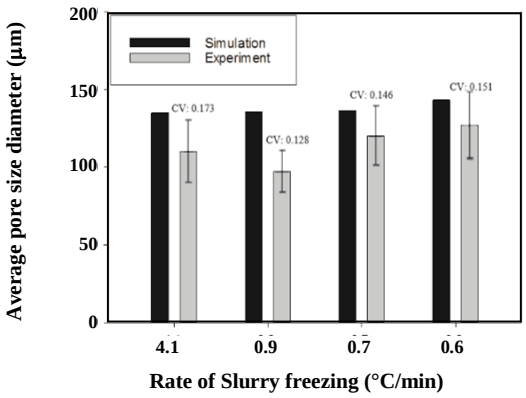

Fig. 9: Comparison between the experimental [3] and calculated average pore size of the scaffold for different cooling rates.

on the temperature in which the slurry nucleated at the different areas within the mold [16]. To study the effect of nucleation temperature and slurry filling height on the scaffold pores size, the conditions of the freezing process were set as reported by *Pawelec et al.* [16], Table 2, with considering two different T_n (–10 and –3 °C). When T_n was set to –10 °C, the results showed the existence of slim layers of larger pores near mold walls in all three different filling heights of the slurry, 10, 15 and 20 mm (Fig. 12(a), (c) and (e). In this case, the average pore size increased steadily, as the slurry filling height increased which was the direct result of the freezing time extension.

When T_n was set to –3 °C, a different trend in pore/crystal size distribution was observed for three slurry filling heights. Fig. 12 shows that by increasing the slurry filling height at higher nucleation temperature, –3 °C, a region of bigger pore/crystal size began to develop at the top of the slurry which was in accordance with the experiment reported earlier [16] (Fig. 12(b), (d) and (f)). In comparison to filling height at a lower T_n, –10 °C, the top of the scaffold was affected more through higher nucleation (i.e. T_n = –3 °C). From Fig. 12(b), (d) and (f), it can be seen that pore size at the top of the scaffold increased considerably through increasing the slurry filling height within the mold. In agreement

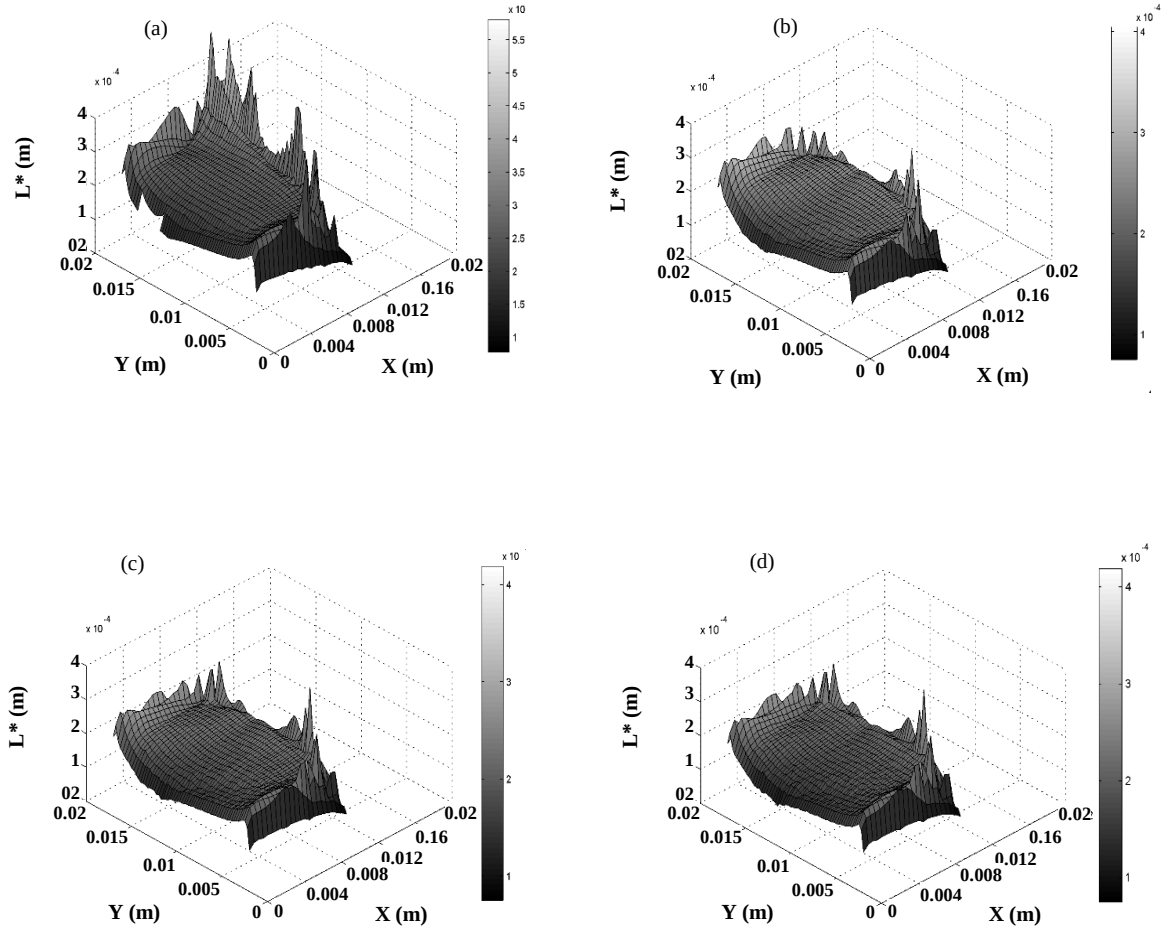

Fig. 10: Pore size distribution at different set freezing points: (a) –10 °C, (b) –20 °C, (c) –30 °C, and (d) –40 °C.

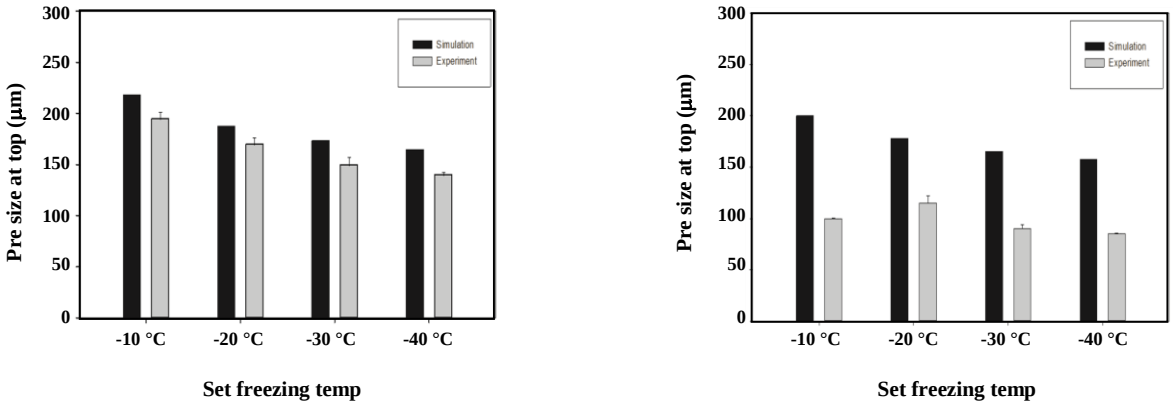

Fig. 11: Comparison between experimental average pore size reported by Pawelec et al. [17] and predicted results (similar conditions of mold and cooling as the work of Pawelec et al. were considered).

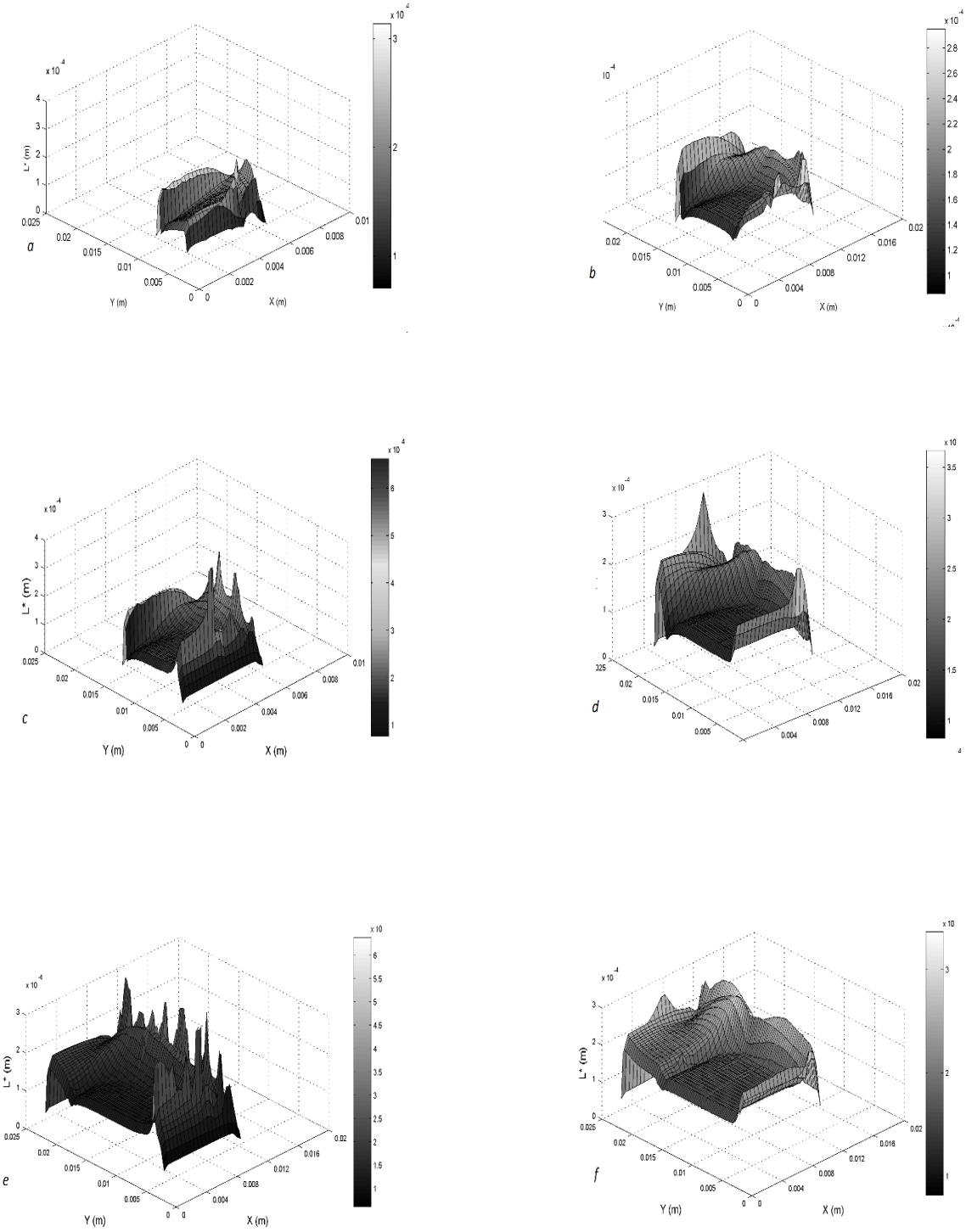

Fig. 12: Effect of the slurry height (H) and nucleation temperature (T_n) on the scaffold structure: (a) T_n = -10°C & H = 10 mm (b) T_n = -3°C & H = 10 mm (c) T_n = -10°C & H = 15mm (d) T_n = -3°C & H =15 mm (e) T_n = -10°C & H = 20 mm (f) T_n = -3°C & H = 20 mm

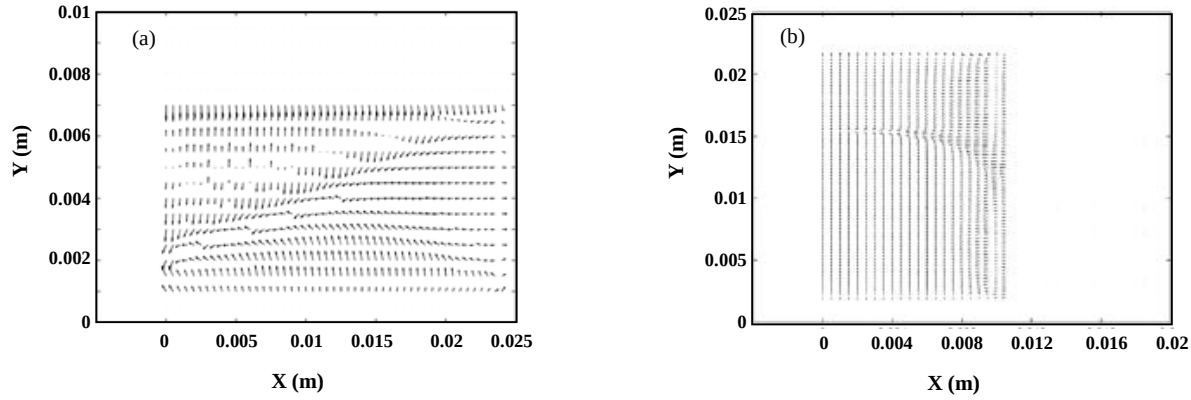

Fig. 13: Temperature gradient vector in (a) mold with thin aluminum side wall (T_n = –7 °C, mold height = 1 cm and side wall =1 mm), (b) mold with thick insulated sidewall (T_n = –3 °C, mold height = 2 cm and sidewall=1 cm)

with the experimental data, the final scaffold was composed of two different parts; the bottom included smaller pores and the top with greater pores, the latter, then, grew in size by raising the filling height [17, 21].

The amount of the latent heat generated through crystallization was taken out by means of the convection from the top and bottom of the mold, which was swifter in steel mold bottom, owing to higher thermal diffusivity and convection heat transfer coefficient of steel compared to air (See Table 1). Since the top of the slurry was in contact with air, it had lower heat transfer rate compare to the bottom of the slurry which was in contact with the mold's steel bottom. Increasing slurry filling height would lower the effect of higher heat transfer rate of the bottom, insulating the top. This would result in increasing the solidification time, t_s, at the top which would increase the crystal/pore size at this region.

The formation of bigger pores in the higher nucleation temperature at the top of the scaffold was mainly due to lower temperature gradient between the slurry and the top air. Comparing the results of mean pore size for filling height of 20 mm at two different T_n (Fig (e) and (f)) indicates that the top was cooled slowly at T_n = –3 °C, increasing freezing time and pore/crystal size.

The effect of thermal gradient

As mentioned before, two factors in crystallization affect the crystal size and shape; namely freezing time, and thermal gradient, t_s and G, respectively. Being a vector, G has direction in addition to magnitude. The direction of G was calculated through summation of thermal differences between an element and its four adjacent elements.

In order to investigate crystal orientation, thermal gradient vectors during crystallization were calculated for two different experiments and the results were compared; This included thermal gradients of the slurry in the mold with thin aluminum side wall in our experiment and in the mold with thick insulated sidewall of *Pawelec et al.* [17]. It was attained through Fig. 13 that the orientation pattern in the thick insulated mold wall, was much less chaotic than in our metallic thin wall mold, although in both cases, the thermal effects of the wall on the pore orientation was still observable near the side wall.

Furthermore, the line of separation between vectors aligned to the scaffold base and its top could be the illustrator of segregation line of oriented pores at the top of the scaffold and the isotropic bottom in reality (see also schematized Figures by *Pawelec et al.* [16]). Experimental results reported by *Pawelec et al.* [16] showed similarly aligned pores at the top with the same mold. In concordance with the experimental data the irregularity can also be seen in the microscopic picture, namely Fig. 1(d).

Fig. 13 (b) reveals that the vectors located at the top, have downward direction while the bottom vectors have opposite direction. As it mentioned before, cooled air at the top and the steel bottom of the mold simultaneously were reducing the temperature of the slurry where the rate of cooling for bottom was more due to higher thermal diffusivity of the steel bed, making the bottom influenced area greater. The growth of a hexagonal ice crystal

in supercooled water is more under the influence of temperature gradient rather than other factors such as stable face of growing ice or surface tension [35]. This can help predict the orientation of spherical shape. Nevertheless, ice crystal growth direction is to be considered in the future research.

CONCLUSIONS

A code based on the finite element method was developed to predict the final scaffold structure made by freeze-drying method and study the effect of material and processing parameters on the microstructure of the resulted scaffold. It was shown that nucleation temperature (T_n) had different impact on the scaffold structure depending on the mold material. It was shown that in polystyrene (PS) molds, T_n had no significant effect while in aluminum (Al) mold, it drastically changed the scaffold structure resulting in bigger pore sizes in Al mold. It was believed that it was the direct result of higher heat conductivity of aluminum which assisted the generated heat to be transferred into greater area within the mold homogenizing the temperature distribution. The effect of the cooling rate and set freezing temperature were also investigated. It was depicted that increasing cooling rate would result in smaller pore sizes. It was also found that the slurry height in the mold had great impact on the scaffold structure at higher nucleation temperatures (T_n). It was concluded that nucleation temperatures (T_n) was an effective parameter controlling the microstructure of the scaffolds prepared through the freeze-drying process. Since this parameter was not controllable, measures such as using PS mold or reduced height of slurry should be considered to reduce the effect of T_n on the scaffold structure and control the final microstructure, as proposed in the present study [36].

Acknowledgment

The authors gratefully acknowledge Mr. C R Muzzio for his helpful assistance.

Received : Dec. 7, 2018 ; Accepted : May 13, 2019

REFERENCES

[1] Chung H.J., Park T.G., Surface Engineered and Drug Releasing Pre-Fabricated Scaffolds for Tissue Engineering. *Advanced Drug Delivery Reviews*, **59**(4): 249-262 (2007).

[2] O'Brien F.J., Biomaterials & Scaffolds for Tissue Engineering. *Materials Today*, **14** (3): 88-95 (2011).

[3] O'Brien F.J., Harley B.A., Yannas I.V., Gibson L., Influence of Freezing Rate on Pore Structure in Freeze-Dried Collagen-GAG Scaffolds, *Biomaterials*, ***25*** (6), 1077-1086 (2004).

[4] Madaghiele M., Sannino A., Yannas I.V., Spector M., Collagen-Based Matrices with Axially Oriented Pores, *Journal of Biomedical Materials Research Part A*, **85** (3): 757-767 (2008).

[5] Alizadeh M., Abbasi F., Khoshfetrat A., Ghaleh H., Microstructure and Characteristic Properties of Gelatin/Chitosan Scaffold Prepared by a Combined Freeze-Drying/Leaching Method, *Materials Science and Engineering: C*, **33**(7): 3958-3967 (2013).

[6] Davidenko N., Gibb T., Schuster C., Best S.M., Campbell J., Watson C., Cameron R.E., Biomimetic Collagen Scaffolds with Anisotropic Pore Architecture, *Acta Biomaterialia*, **8** (2): 667-676 (2012).

[7] Haugh M.G., Murphy C.M., O'Brien F.J., Novel Freeze-Drying Methods to Produce a Range of Collagen–Glycosaminoglycan Scaffolds with Tailored Mean Pore Sizes, *Tissue Engineering Part C: Methods*, **16** (5): 887-894 (2009).

[8] Yuan N.-Y., Lin Y.-A., Ho M.-H., Wang D.-M., Lai J.-Y., Hsieh H.-J., Effects of the Cooling mode on the Structure and Strength of Porous Scaffolds Made of Chitosan, Alginate, and Carboxymethyl Cellulose by the Freeze-Gelation Method, *Carbohydrate Polymers*, **78** (2): 349-356 (2009).

[9] Tanthapanichakoon W., Tamon H., Nakagawa K., Charinpanitkul T., Synthesis of Porous Materials and Their Microstructural Control through Ice Templating. *Engineering Journal*, **17** (3): 1-8 (2013).

[10] Moore M.J., Friedman J.A., Lewellyn E.B., Mantila S.M., Krych A.J., Ameenuddin S., Knight A.M., Lu L., Currier B.L., Spinner R.J., Multiple-Channel Scaffolds to Promote Spinal Cord Axon Regeneration, *Biomaterials*, **27** (3): 419-429 (2006).

[11] Yannas I., Burke J., Orgill D., Skrabut E., Wound Tissue can Utilize a Polymeric Template to Synthesize a Functional Extension of Skin, *Science*, **215** (4529): 174-176 (1982).

[12] Lee S.Y., Oh J.H., Kim J.C., Kim Y.H., Kim S.H., Choi J.W., In vivo Conjunctival Reconstruction Using Modified PLGA Grafts for Decreased Scar Formation and Contraction, *Biomaterials*, **24**(27): 5049-5059 (2003).

[13] Murphy C.M., Haugh M.G., O'Brien, F.J., The Effect of Mean Pore Size on Cell Attachment, Proliferation and Migration in Collagen–Glycosaminoglycan Scaffolds for Bone Tissue Engineering. *Biomaterials*, **31** (3): 461-466 (2010).

[14] Berry C.C., Campbell G., Spadiccino A., Robertson M., Curtis A.S., The Influence of Microscale Topography on Fibroblast Attachment and Motility, *Biomaterials*, **25**(26): 5781-5788 (2004).

[15] Woinet B., Andrieu J., Laurent M., Min S., Experimental and Theoretical Study of Model Food Freezing. Part II. Characterization and Modelling of the Ice Crystal Size, *Journal of Food Engineering*, **35**(4): 395-407 (1998).

16] Pawelec K., Husmann A., Best S.M., Cameron R.E., Understanding Anisotropy and Architecture in Ice-Templated Biopolymer Scaffolds, *Materials Science and Engineering: C*, (2014).

[17] Pawelec K., Husmann A., Best S.M., Cameron R.E., A Design protocol for tailoring ice-templated scaffold Structure, *Journal of the Royal Society Interface*, **11**(92): 20130958 (2014).

[18] Kiani H., Sun D.-W., Water Crystallization and Its Importance to Freezing of Foods: A Review, *Trends in Food Science & Technology*, **22**(8): 407-426 (2011).

[19] Lunardini, V.J., "Heat Transfer with Freezing and Thawing", Elsevier: (1991).

[20] Moore E.B., Molinero V., Structural Transformation in Supercooled Water Controls the Crystallization Rate of Ice, *Nature*, **479**(7374): 506-508 (2011).

[21] Nakagawa K., Hottot A., Vessot S., Andrieu J., Modeling of Freezing Step during Freeze-Drying of Drugs in Vials, *AIChE Journal*, **53**(5): 1362-1372 (2007).

[22] Saatchi, A., Seddiqi, H., Amoabediny, G., Helder, M.N., Zandieh-Doulabi, B., Klein-Nulend, J., Computational Fluid Dynamics in 3D-Printed Scaffolds with Different Strand-Orientation in Perfusion Bioreactors. *Iranian Journal of Chemistry and Chemical Engineering (IJCCE)*, - (2019). [in Press]

[23] Muzzio C.R., Dini N.G., Simulation of Freezing Step in Vial Lyophilization Using Finite Element Method, *Computers & Chemical Engineering*, **35** (11): 2274-2283 (2011).

[24] Nakagawa, K., Thongprachan, N., Charinpanitkul, T., Tanthapanichakoon, W., Ice Crystal Formation in the Carbon Nanotube Suspension: A Modelling Approach, *Chemical Engineering Science*, **65** (4): 1438-1451 (2010).

[25] Quintero Ortega I.s.A., Mota-Morales J.D., Elizalde Peña E.A., Zárate-Triviño D.G., De Santiago Y.A., Ortiz A., García Gaitan B., Sanchez I.C., Luna-Bárcenas G., Cryogenic Process to Elaborate Poly (ethylene glycol) Scaffolds. Experimental and Simulation Studies. *Industrial & Engineering Chemistry Research*, **52** (2): 706-715 (2012).

[26] Chan K., Liang W., Francis W., Nicolella D., A Multiscale Modeling Approach to Scaffold Design and Property Prediction, *Journal of the Mechanical Behavior of Biomedical Materials*, **3**(8): 584-593 (2010).

[27] Hollister S., Maddox R., Taboas J., Optimal Design and Fabrication of Scaffolds to Mimic Tissue Properties and Satisfy Biological Constraints, *Biomaterials*, **23**(20): 4095-4103 (2002).

[28] Mehdizadeh H., Sumo S., Bayrak E.S., Brey E.M., Cinar A., Three-dimensional Modeling of Angiogenesis in Porous Biomaterial Scaffolds, *Biomaterials*, **34** (12): 2875-2887 (2013).

[29] Yu P., Lee T.S., Zeng Y., Low H.T., Fluid Dynamics and Oxygen Transport in a Micro-Bioreactor with a Tissue Engineering Scaffold, *International Journal of Heat and Mass Transfer*, **52** (1): 316-327 (2009).

[30] Youssef K., Mack J., Iruela-Arispe M., Bouchard L.S., Macro-Scale Topology Optimization for Controlling Internal Shear Stress in a Porous Scaffold Bioreactor, *Biotechnology and Bioengineering*, **109**(7): 1844-1854 (2012).

[31] Kamalipour M., AliMousavi Dehghani S.A., Naseri A., Abbasi S., Distinguishing Anhydrate and Gypsum Scale in Mixing Incompatible Surface and Ground Waters During Water Injection Process, *Iranian Journal of Chemistry and Chemical Engineering (IJCCE)*, **37**(1): 231-240 (2018).

[32] Jamshidi S., Bozorgmehry Boozarjomehry R., Pishvaie S.M.R., An Irregular Lattice Pore Network Model Construction Algorithm, *Iranian Journal of Chemistry and Chemical Engineering (IJCCE)*, **29**(1): 61-70 (2010).

[33] Ghaleh H., Abbasi F., Alizadeh M., Khoshfetrat A.B., Mimicking the Quasi-Random Assembly of Protein Fibers in the Dermis by Freeze-Drying Method, *Materials Science and Engineering: C*, **49**: 807-815 (2015).

[34] Williams T.L., "An Experimental Investigation of Natural Convection Heat Transfer in a Refrigerator During Closed Door Conditions"; Air Conditioning and Refrigeration Center. College of Engineering, University of Illinois at Urbana-Champaign (1994).

[35] Shultz, M.J., Bisson, P.J., Brumberg, A., Best Face Forward: Crystal-Face Competition at the Ice-Water Interface, *The Journal of Physical Chemistry B*, **118**(28): 7972–7980 (2014).

[36] Swope W.C., Andersen H.C., Berens P.H., Wilson K.R., A Computer Simulation Method for the Calculation of Equilibrium Constants for the Formation of Physical Clusters of Molecules: Application To Small Water Clusters, *The Journal of Chemical Physics*, **76**(1): 637-649 (1982).